Epitaxial growth of 3,4,9,10-perylene-tetracarboxylic-dianhydride on Au(111): A STM and RHEED study

T. Schmitz-Hübsch, T. Fritz, F. Sellam, R. Staub, and K. Leo
Institut für Angewandte Photophysik, Technische Universität Dresden, D-01062 Dresden, Germany
(Received 8 November 1996)

The crystal structure of 3,4,9,10-perylene-tetracarboxylic-dianhydride (PTCDA) grown by organic molecular-beam epitaxy on reconstructed Au(111) surfaces is investigated by scanning tunneling microscopy and reflection high-energy electron diffraction. Large domains of PTCDA (up to 200 nm) are found on the still reconstructed Au surface. The reconstruction can be used to precisely determine the lattice orientation of the PTCDA layers. Three different orientations with respect to the gold substrate were observed. All of them can be explained in terms of a point-on-line growth model that was originally proposed for explaining organic epitaxy results on graphite. [S0163-1829(97)04612-2]

I. INTRODUCTION

Recently, much interest has been focused on thin organic films due to their potential applicability for electronic and optoelectronic devices such as organic light-emitting diodes, optical detectors, and waveguides. Of particular interest is the growth of well-ordered organic films on inorganic single-crystalline substrates and the investigation of the relation between substrate orientation and film structure. Of the various substances used for previous studies of organic molecular-beam epitaxy (OMBE), much work has been focused on the growth of 3,4,9,10-perylene-tetracarboxylic-dianhydride (PTCDA) on different crystalline substrates[1–8] since this molecule exhibits interesting optical and electronic properties. Furthermore, the brick-shaped PTCDA molecule easily forms well-ordered films on various substrates due to its unique crystal structure that is characterized by flat-lying molecules in the (102) plane of the bulk.[1]

Here, we report on the structural properties of highly ordered PTCDA layers on Au(111) as determined by scanning tunneling microscopy (STM) and reflection high-energy electron diffraction (RHEED). The combination of the diffraction method (RHEED) with the ultrahigh resolution of STM is a suitable way of exploring the crystalline structure of grown overlayers and can—at least partially—overcome the limitations of both surface analysis techniques: the STM can provide basic data about the molecular alignment within the unit cell, information that cannot be drawn from the diffraction pattern. However, because of unavoidable head drift and scaling errors, the STM data are usually only of limited accuracy. Also, the imaging is limited to a small area if submolecular resolution is desired. The advantage of RHEED on the other hand, is to allow for real *in situ* investigation during the film growth. For our study, a metal (epitaxial gold films on mica) has been chosen as substrate because most of the prospective applications mentioned above require metal electrodes. Furthermore, gold is a very suitable substrate for STM investigations and the gold films exhibit large atomically flat terraces.[9,10]

II. EXPERIMENT

Our experimental setup for the OMBE consists of three interconnected UHV chambers for sample preparation, epitaxy process, RHEED, and STM/AFM investigation, respectively. For quick refill of organic materials the Knudsen cells are equipped with a load-lock mechanism.

The gold surfaces were prepared under UHV conditions by evaporation of gold onto freshly cleaved mica (0001) surfaces. Under elevated substrate temperature (800 K) and high evaporation rates (ca 0.5 nm/s) this process leads to epitaxial gold films with a terrace width of typically 200 nm.[9,10] These terraces exhibit the well-known $(22\times\sqrt{3})$ reconstruction with alternating fcc- and hcp-domains, separated by domain walls running along the Au$[\bar{1}\,\bar{1}2]$ direction with a period of 63.45 Å.[11] The PTCDA molecules were deposited at various substrate temperatures (300–450 K) at a rate of approximately two monolayers (ML) per minute as determined by a quartz balance. During the deposition, the Knudsen cell was held at 650 K and the pressure was in the range of 8×10^{-10} mbar. The PTCDA (Aldrich) was previously purified by gradient sublimation. The STM images were taken *in situ* by a combined STM/AFM (Omicron) as well as under ambient conditions using a NanoScope II (Digital Instruments). Structural data were obtained during the deposition using a RHEED system with a charge-coupled device (CCD) camera (Staib Instruments). To inhibit degradation of the PTCDA films under high-energy electron bombardment, the measuring time was kept small (10 s) and the beam was blanked out most of the time. No damage of the films has been observed under these conditions.

To enhance the visibility of the weak streaks of PTCDA, the recorded image is averaged in the streak direction (i.e., horizontal) and then differentiated in the direction perpendicular to the streaks. Next, the streak position is determined automatically by a numerical procedure in each *horizontal* line in order to objectify the data analysis. Then, the total number of peak positions found in each *vertical* line is calculated, regardless of the actual peak intensity. In this way, a histogram of the most-likely peak positions in the entire image is generated. This algorithm advantageously compares to ordinary intensity profiles, because less intense peaks can contribute likewise to the result, if only a distinguishable peak is found at the same position in a sufficiently large number of horizontal image lines. Of course, this procedure

requires a strict vertical alignment of the RHEED streaks, which can be easily obtained by turning the CCD camera in the camera holder.

III. RESULTS AND DISCUSSION

Figure 1(a) shows a typical RHEED image, taken at a PTCDA coverage of 1–2 ML. As in previous RHEED studies of PTCDA on highly oriented pyrolytic graphite (HOPG) (Ref. 5) and Au(111), (Ref. 6) a variety of rather weak Bragg reflexes, stemming from the PTCDA lattice, can be seen. At this low coverage, the diffraction streaks of the Au[110] lattice rods are still visible as the bright lines in the image. The observed patterns are nearly independent of the rotation angle, i.e., substrate orientation. Nevertheless the streaks are narrow and elongated, which proves good crystallinity of the grown layer. The pattern remains unchanged during further growth, and we do not find a significant relaxation of the lattice parameters from a monolayer up to a layer thickness of 10 nm. The Bragg spacings and the errors obtained from the processed RHEED pattern [Fig. 1(b)] are shown in Fig. 1(c). Here, the known lattice period in the Au⟨110⟩ azimuth (2.498 Å) is used to accurately calibrate the images.

To understand the complexity of the observed RHEED images and to deduce the lattice parameters, additional information about the molecular arrangement in the films is required. This information can be provided by STM: It is visible from the image shown in Fig. 2(a) that PTCDA layers on gold grow in a two-dimensional fashion similar to the (102) plane of the molecular crystal,[1] forming a rectangular lattice with two flat-lying molecules per unit cell. Because neither RHEED nor STM data reveal any information about the growth into the direction perpendicular to the substrate, we express in the following analysis of the observed RHEED patterns the azimuths of the PTCDA layers with the lattice vectors of the two-dimensional unit cell of the (102) plane of β-PTCDA, i.e., using two indices instead of three as depicted in Fig. 2(b).

If the STM results are taken into account, it is obvious that the obtained RHEED patterns consist of streaks that belong to different azimuthal orientations of these PTCDA (102) planes. In order to assign the measured spacings to certain azimuthal orientations, we have calculated the RHEED images for all low-indexed directions $[hk]$ $(0 \leqslant h,k \leqslant 5)$, assuming the lattice constants are close to α- and β-PTCDA.[1] The calculations were carried out with RHEED simulation software (Staib Instruments) especially designed to compute RHEED patterns of organic crystals in the kinematic approach. Details about the simulation will be published elsewhere. The suggested indexing of the azimuthal directions is summarized in Fig. 1(c). In disagreement with the assignment of Fenter *et al.*[6] the streak at 4.61 Å is assigned to the (14) lattice rod. This is done since our computer simulations show that this reflex would appear at around 4.5 Å and is much brighter than the (22) reflex, which is expected to appear at about 5.3 Å.

Finally, the lattice parameters of the two-dimensional lattice are determined from that set of data by using a nonlinear least-square-fit algorithm. The obtained parameters are $a=12.2\pm0.2$ Å, $b=19.7\pm0.4$ Å, and $\Gamma=(90\pm2)°$, but do not allow us to clearly classify the lattice as either α- or

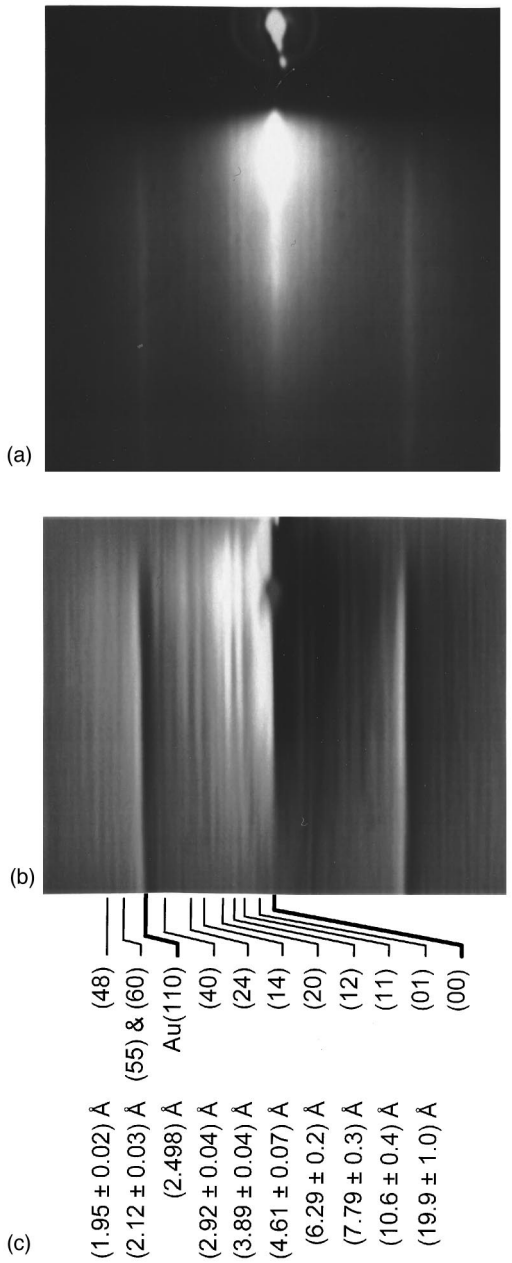

FIG. 1. (a) RHEED image of 1–2 ML of PTCDA on Au(111) taken in the Au(110) azimuth at 12 kV and ~3° incident angle. The second image (b) is differentiated for clarity. The diffraction streaks of gold are used for calibration. (c) Diagram of the observed diffraction streaks, their spacings, and their assignment to Bragg lines of the two-dimensional lattice of the PTCDA (102) plane.

β-PTCDA or to establish a new modification. Within error, these values are similar to those found previously.[6] The problem of rather large error bars is inherent to the application of RHEED to organic solids with large lattice constants: it is found that even in a screen filling CCD image (512×512 pixels) an uncertainty in the position of the RHEED streaks of only 1 pixel would cause an error of approximately ±0.5 Å for the largest Bragg spacings.

We now address the question of both the orientation and the number of nonequivalent PTCDA domains with respect to the gold substrate. Fenter *et al.*[6] assumed that the [21]

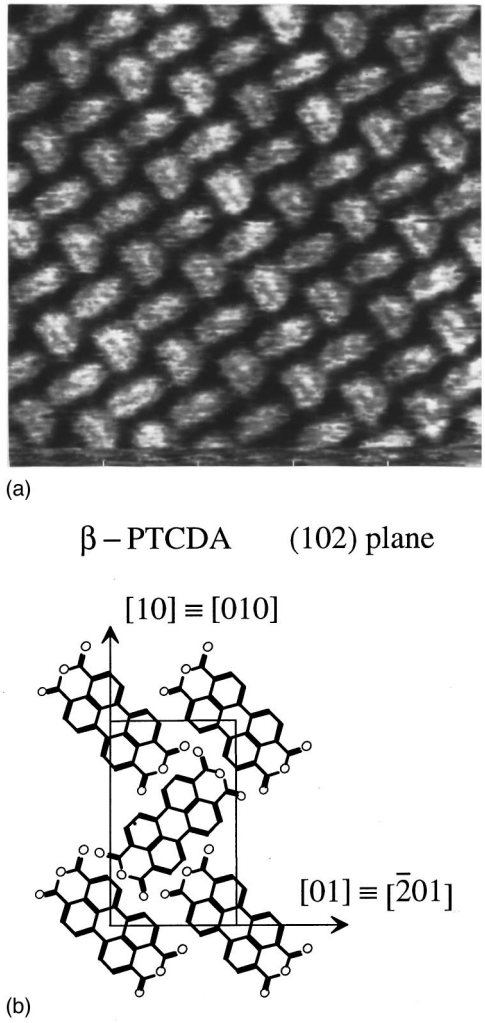

FIG. 2. (a) STM image (10×10 nm^2) of PTCDA on Au(111) taken with the Omicron STM/AFM in constant height mode at 100 mV, 3 nA. PTCDA growths with the (102) plane parallel to the substrate. (b) Arrangement of the PTCDA molecules in the (102) plane and definition of the two-dimensional rectangular lattice.

direction of the two-dimensional PTCDA lattice always coincides with the [110] axis of gold. This would mean that the observed RHEED pattern consists of an incoherent superposition of the six *equivalent* domains of PTCDA. Since the [14] and [41] direction of PTCDA appear at an angle of about $\pm60°$ to the [21] direction, a superposition of only these particular azimuths should be observed. This is obviously not the case, and thus indicates the existence of additional PTCDA domains that must have different orientations with regard to the Au[110] direction.

From gracing incident x-ray diffraction it is already known that the Au(111) surface reconstruction is not lifted during deposition of PTCDA.[6] This is clearly seen in all of our STM images where the reconstruction lines remain visible as a modulation of the image contrast. We take advantage of this fact to eliminate possible drift and distortion in the STM images by using the reconstruction period as a *built-in* scale. In practice, this is done in Fourier space, where the reciprocal unit cell of both the Au reconstruction and PTCDA can be easily measured. Since the reconstruction lines are known to run along the [1$\bar{1}$2] direction, they

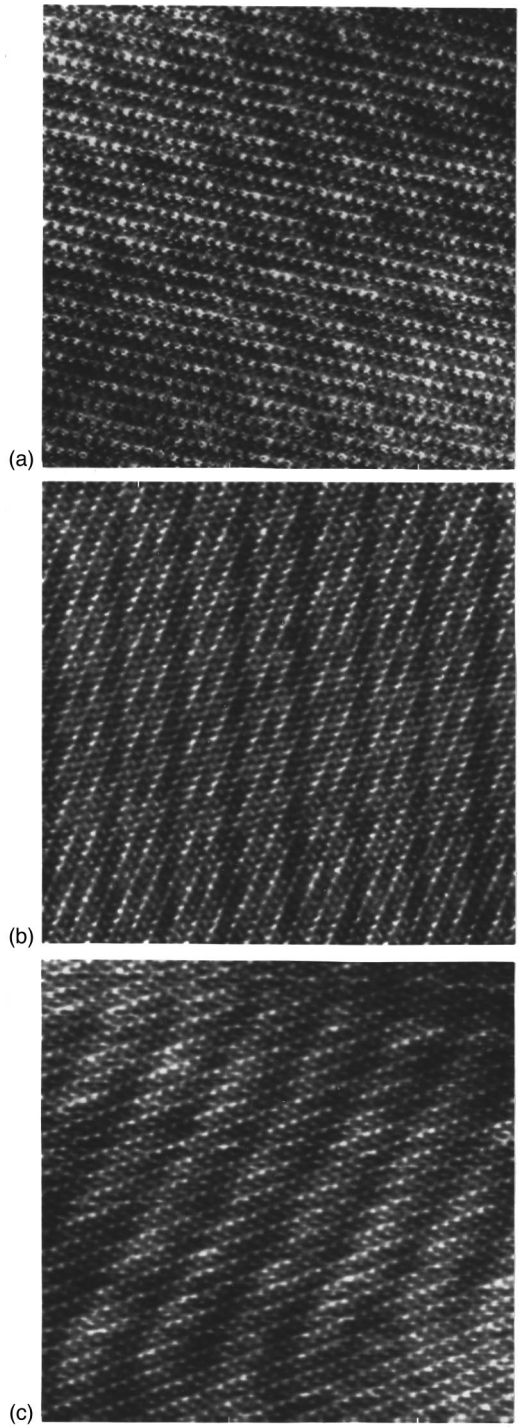

FIG. 3. STM images (50×50 nm^2) of different domains of PTCDA on Au(111). All images show the presence of the Au($22\times\sqrt{3}$) reconstruction as a modulation of molecular contrast. Orientation of the [10] axis of the PTCDA lattice to the reconstruction lines, i.e., the [1$\bar{1}$2] direction of gold: (a) 55°, (b) 22°, and (c) 39°. The images are taken in constant current mode at 200 mV, 1.5 nA with the Nanoscope II.

allow us to determine the orientation of the two-dimensional PTCDA lattices with respect to the substrate. An important experimental finding is that three basically different lattice alignments exist, as can be directly seen from the STM images shown in Fig. 3. The different orientations are listed in Table I. While the reconstructed Au(111) surface has a two-

TABLE I. Calculated misfit values for various orientations $d(hk)$. The orientation angles found in the STM images are in good agreement with the angles predicted for minimal misfit values. For orientations marked with an asterisk, both molecules of the unit cell lie on the lattice lines, for the other orientations only one molecule fulfills this condition. See the text for the definition of the misfit and for used lattice parameters.

			Angle $[10]_{PTCDA}$ to $[\bar{1}\bar{1}2]_{Au}$	
Orientation	$d(hk)$ (Å)	Misfit	Calculated	Measured
$d(44)$*	2.59	7.22%	29.1°	
$d(36)$	2.55	5.39%	9.8°	
$d(27)$	2.54	5.27%	4.2°	
$d(08)$*	2.45	1.32%	28.9°	
$d(\bar{5}0)$	2.44	1.09%	61.1°	
$d(\bar{5}1)$*	2.42	0.31%	54.0°	(55±2)°
$d(\bar{4}5)$	2.41	−0.34%	23.2°	(22±2)°
$d(\bar{1}8)$	2.40	−0.66%	40.2°	(39±2)°
$d(52)$	2.37	−1.92%	47.1°	
$d(37)$*	2.31	−4.57%	5.6°	
$d(53)$*	2.29	−5.32%	40.6°	
$d(28)$*	2.27	−5.96%	−7.1°	
$d(46)$*	2.23	−7.72%	18.0°	
$d(54)$	2.1852	−9.54%	28.9°	

fold symmetry locally, it itself exists in three possible domains. Thus the total number of possible PTCDA orientations is 18. The structure models of the observed domains are displayed in Fig. 4. This finding explains why we do not observe a pronounced angle dependence in the RHEED experiments as reported for other organic films[12] but instead find streaks belonging to PTCDA domains of different orientation at a fixed angle.

For all observed orientational domains, it is found that the PTCDA lattice neither follows the herringbonelike superstructure of the uniaxial compressed reconstruction nor is distorted significantly at the domain boundaries of the reconstruction (a distortion would lead to elongated spots or double spots in the Fourier transformation of the image). This strongly indicates *that the corrugation potential seen by the PTCDA molecules is small compared to the lattice potential of PTCDA.*

We can thus assume that the point-on-line epitaxy concept proposed by Hoshino *et al.*[2,13] should be applicable to explain the observed domains of PTCDA. The concept is based on the assumption that the structure of the organic film is basically the same as in the bulk and only slight distortion due to the deposit-substrate interaction is possible. Then, the deposited organic film grows in such a way that all lattice points of the deposit lie on lattice lines of the substrate. In other words d_{hk} of the deposit coincides with d_s of the substrate, were d_{hk} denotes the distance of the (hk) lines of the deposit and d_s the distance of the principal lattice lines of the substrate. The possible pairs (h,k) and thus the orientation belong to a minimal misfit defined as $100\times(d_{hk}-d_s)/d_s$.[13]

Compared to the unreconstructed Au(111) surface where $d_{\mathrm{Au}(\bar{1}10)}=\sqrt{(3/8)}a_{\mathrm{Au}}=2.498$ Å, the corresponding distance $d=\cos(\varphi)(22/23)d_{\mathrm{Au}(\bar{1}10)}=2.416$ Å ($\varphi=\arctan[22/(23\sqrt{3})]$) is smaller on the reconstructed surface (see also Fig. 4). Table I compares the various orientations (misfit≤10%) and the orientations found in the STM images. The experimentally observed orientations are in *good agreement with those belonging to minimal misfit values*. It is important to note that only for the first observed domain both molecules of the unit cell lie on a lattice line. Nevertheless, the total misfit for the other two domains seems to be small enough to stabilize these orientations. One can speculate whether this is the reason for the different contrast of the two molecules in the unit cell as observed in the STM images of these particular domains. The question whether some of the domains are commensurate in higher order [e.g., (3×1) coincidence for the third domain] cannot be decided by STM.

In summary, we have shown the existence of three different crystalline domains of PTCDA on the reconstructed Au(111) surface. They differ in their orientation to the Au substrate and possibly also slightly in their lattice constants.

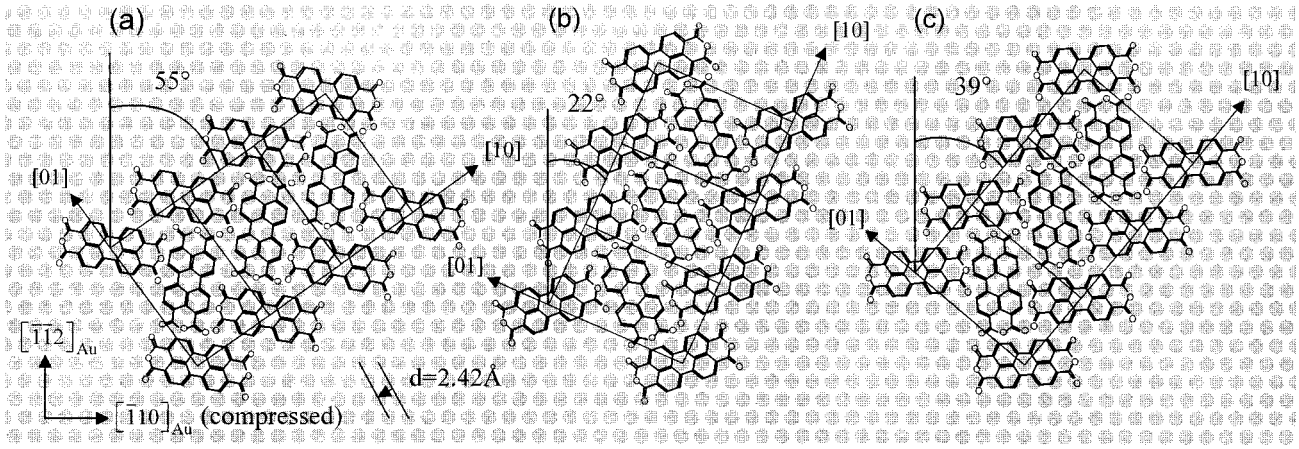

FIG. 4. Schematic drawing of the observed orientations of the two-dimensional PTCDA lattice on the reconstructed Au(111) surface. The gold lattice is compressed by the factor of 22/23 (4.35%) along the [110] direction. All three domains show point on line coincidence, at least for the molecules on the corner of the unit cell. The PTCDA molecules are not exactly to scale.

The latter case cannot be confirmed with STM since the deviations are expected to be in the range of 2%. All experimentally observed domains are predicted by the point-on-line epitaxy model. This shows that this special lattice matching mode is not limited to the growth of organic compounds on HOPG but seems to be a general feature for the growth of organic-inorganic interfaces whenever the corrugation potential is sufficiently small.

ACKNOWLEDGMENTS

The authors are grateful to N. Karl, University of Stuttgart, for helpful discussions of the RHEED results, P. Miskowiec for help with the RHEED simulations, and E. Erler for technical support. This work has been supported by the Bundesministerium für Bildung, Wissenschaft, Forschung und Technologie under Grant No. 13N6263.

[1] M. Möbus, N. Karl, and T. Kobayashi, J. Cryst. Growth **116**, 495 (1992).

[2] A. Hoshino, S. Isoda, H. Kurata, and T. Kobayashi, J. Appl. Phys. **76**, 4114 (1994).

[3] C. Ludwig, B. Gompf, W. Glatz, J. Petersen, W. Eisenmenger, M. Möbus, U. Zimmermann, and N. Karl, Z. Phys. B **86**, 397 (1992); C. Ludwig, B. Gompf, J. Petersen, R. Strohmaier, and W. Eisenmenger, *ibid*. **93**, 365 (1994).

[4] B. Uder, C. Ludwig, J. Petersen, B. Gompf, and W. Eisenmenger, Z. Phys. B **97**, 389 (1995).

[5] S. R. Forrest, P. E. Burrows, E. I. Haskal, and F. F. So, Phys. Rev. B **49**, 11 309 (1994).

[6] P. Fenter, P. E. Burrows, P. Eisenberger, and S. R. Forrest, J. Cryst. Growth **152**, 65 (1995).

[7] A. Schmidt, T. J. Schurlein, G. E. Collins, and N. R. Armstrong, J. Phys. Chem. **99**, 11 770 (1995).

[8] E. Umbach, C. Seidel, J. Taborski, R. Li, and A. Soukopp, Phys. Status Solidi B **192**, 389 (1995).

[9] J. A. DeRose, T. Thundat, L. A. Nagahara, and S. M. Lindsay, Surf. Sci. **256**, 102 (1991).

[10] T. Fritz, M. Hara, W. Knoll, and H. Sasabe, Mol. Cryst. Liq. Cryst. **253**, 269 (1994).

[11] J. V. Barth, H. Brune, G. Ertl, and R. J. Behm, Phys. Rev. B **42**, 9307 (1990).

[12] A. Koma, Prog. Cryst. Growth Charact. **30**, 129 (1995).

[13] A. Hoshino, S. Isoda, H. Kurata, T. Kobayashi, and Y. Yamashita, J. Appl. Phys. **36**, 4113 (1995).